

Chemical Pressure effect at the boundary of Mott insulator and itinerant electron limit of Spinel Vanadates

P. Shahi¹, A. Kumar¹, Rahul Singh¹, Ripandeep Singh², P.U. Sastry,² A. Das², Amish G. Joshi³, A. K. Ghosh⁴, A. Banerjee⁵ and Sandip Chatterjee^{1,*}

¹Department of Physics, Indian Institute of Technology (Banaras Hindu University),
Varanasi-221 005, India

²Solid State Physics Division, Bhabha Atomic Research Center, Mumbai- 400085 , India

³CSIR-National Physical Laboratory, Dr. K.S. Krishnan Road, New Delhi, India

⁴Department of Physics, Banaras Hindu University, Varanasi-221 005, India

⁵UGC-DAE Consortium for Scientific Research, Indore, Madhya Pradesh- 452017, India

ABSTRACT

The chemical pressure effect on the structural, transport, magnetic and electronic properties (by measuring X-ray photoemission spectroscopy) of ZnV_2O_4 has been investigated by doping Mn and Co on the Zinc site of ZnV_2O_4 . With Mn doping the V-V distance increases and with Co doping it decreases. The resistivity and thermoelectric power data indicate that as the V-V distance decreases the system moves towards Quantum Phase Transition. The transport data also indicate that the conduction is due to the small polaron hopping. The chemical pressure shows the non-monotonous behaviour of charge gap and activation energy. The XPS study also supports the observation that with decrease of the V-V separation the system moves towards Quantum Phase Transition. On the other hand when Ti is doped on the V-site of ZnV_2O_4 the metal-metal distance decreases and at the same time the T_N also increases.

Keywords: Mott Insulator, Magnetization, Spinel Vanadates

INTRODUCTION

Mott insulators are important examples of strongly correlated materials. The strong-coupling limit, $U \gg t$ (U is the inter-atomic Coulomb energy and t is the spin dependent expectation value for the charge transfer between sites), corresponds to materials in which valence electrons are strongly localized in their atomic orbitals (Mott-Hubbard insulator). The opposite weak-coupling limit, $U \ll t$, corresponds to correlated metals whose electrons are completely delocalized (Paramagnetic metal). This implies that a Mott transition is induced at a critical value Uc/t [1]. As a matter of fact, paramagnetic metals and Mott-Hubbard insulators represent two fundamentally different phases that can be interchanged by increasing or decreasing electronic correlations through a first-order quantum phase transition (QPT) [2]. It is highly challenging to characterize the electronic properties of materials when approaching the QPT either from Mott insulator side or from the paramagnetic metal side. Among very few materials, the AV_2O_4 spinels are a family of Mott insulators that fulfil the criterion of varying the t/U ratio because of the metal-metal separation can be changed by applying the chemical pressure i.e., by changing the size of the A^{2+} cation [3]. The absence of e_g electrons makes direct V-V hybridization between t_{2g} orbitals the only relevant contribution to the hopping amplitude. Moreover, t is also a function of the interionic distance, R . This volume dependence between d orbitals is $J/V^{10/3}$ [4], which is the basis of the phenomenological Bloch's equation [5] for magnetic insulators: $\alpha = \partial \ln T_N / \partial \ln V = -3.3$ provided U remains constant. When approached towards itinerant-electron behaviour the α value is very sensitive so that it can indicate the applicability of crystal-field theory [6,7].

ZnV_2O_4 has one of the smallest charge gaps among the vanadium spinels: ($\Delta \approx 0.55$ eV) [8,9]. Therefore, with proper doping on A-site this ZnV_2O_4 may be transferred to the Mott transition. In a recent report [10] a clear evidence of pressure dependence of a nonmonotonic behaviour of charge gap was shown. The nonmonotonic dependence of charge gap on t/U is expected for materials that are deep inside the Mott regime (small t/U ratio) [11,12] and the enhancement of the magnetic up-up-down-down ordering along the $[\pm 1, 0, 1]$ and $[0, \pm 1, 1]$ chains has already been reported in these vanadates [13].

ZnV_2O_4 crystallizes in a cubic spinel structure, where the V atoms form a pyrochlore lattice of corner-sharing tetrahedra. As a matter of fact, the antiferromagnetic (AF) interactions between the V atoms are highly frustrated. At $T_S = 51$ K, ZnV_2O_4 undergoes a structural phase transition where the symmetry is lowered from cubic to tetragonal ($c/a < 1$) with a compression of the VO_6 octahedron along the c axis [14] and the system possibly

orbital orders. This also lifts the geometrical frustration of the cubic phase making way for the second transition at $T_N = 40$ K which is of a magnetic nature and the system orders antiferromagnetically [14-16]. The lattice formed by the V atoms can be described as built up by V-V chains running along the [110], [011], and [101] directions. The magnetic structure, found by neutron diffraction [13,14], is AF along the [110] direction (within the ab plane), but along the [101] and [011] (off plane) directions the V moments order. Moreover, the effective hopping and the $d-d$ transfer integral of ZnV_2O_4 estimated from the X-ray photoemission spectra are close to the metallic LiV_2O_4 [17].

Moreover, it has been shown that in ZnV_2O_4 away from the strong-coupling regime *bond and magnetic* ordering are independent to each other [10]. If the bond ordering is strengthened away from the strong-coupling regime then it may correspond to ferroelectricity as is observed in CdV_2O_4 [18]. It has also been suggested by Kuntscher et al. [10] that ferroelectricity can be increased significantly by decreasing V-V distance as the structural distortion observed in ZnV_2O_4 is identical to CdV_2O_4 . Furthermore, the main limiting factors for ZnV_2O_4 to show spontaneous polarization are the losses or leak currents. The increase in the value of charge gap reduces the losses. In ZnV_2O_4 when external pressure is applied, which lead to the decrease in V-V distance, the charge gap increases above a critical pressure [10]. As the V-V separation decreases the system moves towards the itinerant electron limit [Blanco-Canasa]. Therefore, closing the Mott gap of this geometrically frustrated Mott insulator is a potential route for enhancing ferroelectricity which could be achieved in ZnV_2O_4 by reducing the V-V distance. Chemical substitution is the best way in doing this.

In the present paper we have varied the chemical pressure in ZnV_2O_4 by doping Mn and Co on the Zn site and studied the effect of it on magnetic, optical, transport properties and on electron structure of doped and undoped ZnV_2O_4 . We have also doped Ti on the V site and varied the metal-metal distance and observed its effect. Our results support the universality of the first order character of the transition from the localized to the itinerant-electron and the stabilization of an intermediate phase in which there is a disproportionation into molecular orbitals within clusters and weak bonding between clusters [19,20].

EXPERIMENT

Polycrystalline $(\text{Zn}_{1-x}\text{Mn}_x)\text{V}_2\text{O}_4$, $\text{Zn}_{0.9}\text{Co}_{0.1}\text{V}_2\text{O}_4$ and $\text{Zn}(\text{V}_{1-x}\text{Ti}_x)_2\text{O}_4$ (where $x = 0, 0.05$ and 0.10) were prepared by solid state reaction route. Appropriate ratio of ZnO, CoO, V_2O_3 , Ti_2O_3 and MnO were mixed and pressed into pellets. The pellets were sealed in quartz tube under high vacuum and heat treated into furnace at 800°C for 60 hrs. The X-ray diffraction

measurement was performed at 10K and at room temperature. The magnetic measurements were done with Vibrating Sample magnetometer (VSM). Fourier Transform Infrared Spectroscopy measurements have been done using Spectrum 65 FTIR spectrometer (Perkin Elmer Instruments, USA) in the range of 500 to 4000 cm^{-1} . Resistivity measurements has been performed by four probe method and thermoelectric power measurement (Seebeck coefficient) has been done using home-made thermoelectric setup. X-ray Photoelectron Spectroscopy (XPS) experiments were performed using Omicron Nanotechnology UHV system equipped with a twin anode Mg/Al X-ray source (DAR400), a monochromator and a hemispherical electron energy analyzer (EA125 HR). All the XPS measurements were performed inside the analysis chamber under base vacuum of 5.0×10^{-10} Torr using monochromatized $\text{AlK}\alpha$. The total energy resolution, estimated from the width of the Fermi energy, was about 300 meV for monochromatic $\text{AlK}\alpha$ line with photon energy 1486.60 eV.

RESULTS & DISCUSSION

The XRD measurement of all the samples indicates the single phase nature of the samples. The samples crystallize in cubic phases with $Fd-3m$ space group. At low temperature (structural transition temperature) the structure changes to tetragonal phase with $I41/a$ space group. We have refined the diffraction data using the Fullprof program (shown in Fig.1) and the fitted parameters are shown in Table-I. In the inset of Fig. 1 the X-ray diffraction pattern of Mn and Ti doped samples have been shown in a very narrow 2θ (61.5° - 63°) range at 300K (above the structural transition) and at 10K (below the structural transition, if any). A very weak splitting is observed for 10% Mn and Co doped samples in the 10K diffraction pattern indicating the decrease of structural distortion. Moreover, for Ti doped samples also structural transition is reduced. The estimated c/a ratio for undoped sample is 0.9892, whereas, for 10% Mn, Co and Ti doped samples it is ~ 0.9894 , ~ 0.9897 and ~ 0.9893 respectively. Magnetization curves of $\text{Zn}_{1-x}\text{A}_x\text{V}_2\text{O}_4$ [$\text{A}=\text{Mn}$ and Co] measured for different doping concentration are shown in Fig.2. For ZnV_2O_4 two clear transitions are observed where the higher temperature is the structural transition and the lower temperature is the magnetic transition [14-16]. It is observed that with increase of doping concentration the peak appears due to structural transition is reduced which is consistent with the XRD measurement.

Figure 3 shows the evolution of T_N with the V-V separation for the $\text{Zn}_{1-x}\text{A}_x\text{V}_2\text{O}_4$ [$\text{A}=\text{Mn}$ and Co] spinels. It is to be mentioned that as the overlap integral in t of $J \propto t^2/U$ [J is the super exchange spin-spin interaction] increases with decreasing R_{V-V} , the energy U must

decrease or remain constant. As a matter of fact, within the localized-electron superexchange, T_N should increase with decreasing V-V separation. In the present investigation it has been observed when Mn is doped the V-V separation increases and subsequently T_N decreases. On the other hand, when Co is doped it is observed that V-V separation decreases very slightly, but interestingly T_N decreases. This suggests that the energy U in the localized electron superexchange theory is not constant when Co is doped.

As mentioned above, the variation of T_N with V-V distance can be interpreted as the consequence of a variation of U/t , which collapses close to the itinerant limit. According to this, even though ZnV_2O_4 and Co-doped ZnV_2O_4 are still semiconducting, a partial electronic delocalization along the V-V bonds may occur as has been anticipated by Pardo et al. [8] for their ZnV_2O_4 and MgV_2O_4 samples which are at the boundary between itinerant and localization limits. In Fig.4 we have shown the experimental resistivity curves for Mn and Co doped and undoped ZnV_2O_4 in which the V-V distances are different. The results show the activation energy decreases with the decrease of V-V distance as the metal-insulator transition is approached from the localized-electron side which confirms the reduction of U/t with decrease of V-V distance, which might be due to a partial delocalization of electrons [3] and in this limit neither the localization-electron model and nor the itinerant-electron model is applicable as has been mentioned by Blanco-canosa et al [3]. It is observed from the resistivity curve at low temperature with the decrease of V-V distances the V^{3+} -3d electrons approaches to the Quantum Phase Transition (QPT) from the localized-electron side. In Fig. 5 the temperature dependence of the thermoelectric power, $S(T)$ is shown for all the spinels mentioned above. The $S(T)$ value is large and positive which indicates that there is only a low density of mobile holes in these vanadates. Thermally activated behaviour of small polarons for all these vanadates is observed. Therefore, the possibility of the existence of the large polaron which forms due to non-stoichiometry can be excluded. Also, the S value decreases from Mn-doped to undoped to the Co-doped ZnV_2O_4 sample.

Moreover, it is observed that ZnV_2O_4 and Co doped ZnV_2O_4 exhibit low activation energy compared to the Mn doped ZnV_2O_4 samples. In consistent with the earlier study [3] a structural transition from the low temperature tetragonal to a high temperature cubic phase is observed. These transitions are due to a co-operative ordering of strong V-V bonding as is observed from XRD refinement. It is found for Mn doped samples the V-V bonding becomes weaker and it moves towards the localized electron side. As is already mentioned that the estimated phenomenological parameter is unfeasible in the Mn-doped samples, therefore, $U \gg t$ might be the case in this Mn doped samples which are in localized electron side.

Furthermore, it is observed in Fig. 2 the susceptibility drops sharply for ZnV_2O_4 and Co-doped ZnV_2O_4 on cooling through the structural transition temperature. This is due to the spin-pairing of V-V bonds [3]. For Mn doped samples this kind of sharp drop is not observed. Furthermore, from the $d\chi/dT$ vs T plot [Fig. 6] it is observed that with increase of Mn content the high temperature peak which is associated with the structural transition is diminished. This behaviour i.e. the suppression of the orbital ordering when it is going towards the Mott-regime ($t \ll U$) is consistent with those already reported [11,12].

We have also measured the transmittance of all the samples and plotted the absorbance as a function of frequency in Fig. 7. A peak is observed below 1000 cm^{-1} which is due to one of the four phonon modes as is observed for cubic spinels. The absorbance spectra show a strong onset above 1000 cm^{-1} . The variation of charge gap (Δ), estimated from the intersection of the linear extrapolation of the absorption edge and the frequency axis, with the inverse of V-V distance is shown in Fig. 8. The Δ initially decreases with increase of V-V distance and with further increase of V-V distance it increases sharply. This non-monotonous behaviour is consistent with that of the external pressure effect [10]. This result we have confirmed by plotting the activation energy (estimated from the resistivity measurement) as a function of inverse V-V distance [Fig. 8]. We have seen that the variation of activation energy with chemical pressure is consistent with that of charge gap variation with chemical pressure. It has already been proposed [8] that in ZnV_2O_4 the V-V dimmers form along the [011] and [101] directions together with an up-up-down-down magnetic order along the same directions. Moreover, in chemical pressure dependence of sample volume [Fig.9] an anomaly is observed for the V-V distance 2.9736 \AA . This is consistent with the inverse V-V distance variation of charge gap data. It might be the fact that stabilization of dimerized phase occurs below the V-V distance 2.9736 \AA . Similar kind of behaviour is observed when 10-12 GPa pressure is applied on ZnV_2O_4 system. Therefore, it might be predicted that 10-12 GPa pressure reduces the V-V distance to 2.9736 \AA . Therefore, we see from the above discussion that T_N , charge gap and activation energy of different spinel vanadates depends on the V-V separation and as it decreases a breakdown of localized electron model for the 3d electrons is observed. This observation is consistent with those observed previously [3,10]. The shortest V-V distance we have obtained in Co doped ZnV_2O_4 and that distance is 2.9738 \AA which is larger than the critical distance for electron itineracy (2.84 \AA) [20]. This is similar to the case of MgTi_2O_4 where a tetramerization of the Ti chains is observed [21].

We have also studied the electronic structure of Mn and Co doped ZnV_2O_4 using x-ray photoemission spectroscopy (XPS). The purpose of this study is to see what happens in the

electronic structures when the system is moving from itinerant electron side to localized electron side and vice versa and to provide clues to understand the origin of charge and orbital orderings in the spinel-type V oxides with tetragonal distortions. Zn 2*p*, V 2*p*, Mn 2*p* and Co 2*p* XPS core-level spectra of ZnV₂O₄, and Mn and Co doped ZnV₂O₄ are shown in Fig. 10. All the core level spectra show 2*p*^{3/2} and V 2*p*^{1/2} states. Both Mn 2*p* and Co 2*p* spectra show satellites peaks. The two clear distinct states of V 2*p*^{3/2} and V 2*p*^{1/2} observed at ~7.6 eV apart, due to spin-orbit splitting. The V 2*p*^{3/2} spectrum of ZnV₂O₄ indicates a V³⁺ single valence level and no indication of the existence of V⁴⁺ (or V⁵⁺) component as has been observed in some other reports [22-24].

Three features (A, B and C) are observed in the valence-band spectra for ZnV₂O₄, and Mn and Co doped ZnV₂O₄ (Fig.11). Feature (A) close to Fermi level (E_F) can be assigned to the antibonding band of the V 3*d* *t*_{2*g*} states hybridized with the O 2*p* states, while features B and C are due to the bonding band of the O 2*p* states hybridized with the V 3*d* *t*_{2*g*} and *e*_g states, respectively [25, 26]. The position of A shifts to the E_F in going from Mn doped ZnV₂O₄ to ZnV₂O₄ to Co doped ZnV₂O₄ and, consequently, the magnitude of the band gap in *t*_{2*g*} bands decreases in this order. The magnitude of the band gap for ZnV₂O₄ ~0.2 eV which is in good agreement with that estimated from the resistivity data. In the case of Co doped ZnV₂O₄, the V 3*d* band reaches very close to E_F , consistent with the resistivity behavior. The binding energy of feature B for Co doped ZnV₂O₄ (4.79 eV), corresponding to the *p*-*d* charge transfer energy, is small compared to those for ZnV₂O₄ and Mn doped ZnV₂O₄ (~5.32 eV).

Takubo *et al.* [17] calculated the tight-binding (TB) parameters for ZnV₂O₄ and CdV₂O₄ using Harrison's rule [27], where the parameters were defined as $(pd\sigma)\alpha 1/(R_{V-O})^{3.5}$, $(dd\sigma)\alpha 1/(R_{V-V})^5$, $(pd\sigma)/(pd\pi)=(dd\sigma)/(dd\pi)=-2.16$ and R_{V-O} and R_{V-V} are the bond lengths between the neighboring V and O sites and between the neighboring two V sites, respectively. The set for the structural parameters and TB parameters are listed in Table II. The $pd\pi$ value for Co doped ZnV₂O₄ (~0.95 eV) is slightly larger than that for ZnV₂O₄ (0.94eV) and Mn doped ZnV₂O₄ (0.93eV). Also it is observed that the $dd\sigma$ value increases slightly in going from Co doped ZnV₂O₄ (-0.52 eV) to ZnV₂O₄ (-0.47 eV) to Mn doped ZnV₂O₄ (-0.40 eV). As a result, the effective hopping due to *d*-*d* transfer $T\sigma=3/4(dd\sigma)$ is ranging from -0.350 eV to -0.356 eV, while the effective hopping due to *p*-*d* transfer $T\pi=-(pd\pi)^2/\Delta$ is ranging from -0.185 eV to -0.21 eV. Here, the values of Δ are estimated from the XPS spectra. This indicates that the exchange interaction due to *d*-*d* transfer is dominant in the systems. The magnitude of T_σ gradually decreases in going from Co doped ZnV₂O₄ to ZnV₂O₄ to Mn doped ZnV₂O₄. The above results show that variations of different

parameters with doping are not so significant. But the tendency clearly indicates that Co-doped ZnV_2O_4 are closer to the itinerant electron limit. Takubo et al.[17] has also shown that for metallic LiV_2O_4 the $pd\pi$ value is larger but $dd\sigma$ value is smaller compared to the semiconducting ZnV_2O_4 and CdV_2O_4 . This also supports our observation.

Takubo *et al.* [17] have explained the XPS for ZnV_2O_4 and CdV_2O_4 by orbital-driven Pierls (ODP) and complex linear combination orbitals (COO) model [28,29]. The ODP scenario is based on the assumptions that the t_{2g} band has one-dimensional character due to the dominant $d-d$ direct hopping and that the t_{2g} band has itinerant character due to the closeness to the metal-insulator transition. The present photoemission study shows the large $dd\sigma$ values indicating the the dominant $d-d$ direct hopping and this increases from Mn doped ZnV_2O_4 to Co doped ZnV_2O_4 through ZnV_2O_4 . Moreover from the above discussion on valence band spectra it is observed that V 3d band reaches closer to the E_F from Mn doped to Co doped ZnV_2O_4 through ZnV_2O_4 . Therefore, when it is going towards the smaller R_{V-V} the Pierls Physics is becoming important over Mott Physics.

In the present investigation we have also doped Ti on the Vanadium site of ZnV_2O_4 to vary the metal-metal distance. It is observed from the refinement of the XRD data that with increase of Ti content the metal-metal distance increases. On the other hand, with increase of Ti content the T_N , charge gap and the activation energy also increase [Figs.12, 13 and 14]. As is already mentioned with localization electron model with increase of metal-metal distance the T_N should decrease. But in the present case as Ti is doped opposite behaviour is observed. It may happen that Ti-doping decreases the intra-atomic Coulomb energy U which in effect increases the T_N . Nevertheless, it deserves further study to explain these interesting phenomena. Moreover, MgTi_2O_4 undergoes a M-I transition on cooling below $T_{MI} \sim 260$ K, accompanied by a strong decrease of the magnetic susceptibility and a transition to a tetragonal structure [30]. The structure in this composition was found to contain dimmers with short Ti-Ti distances (2.85 Å), the locations of the spin singlets. The electronic structure is consistent with the opening of a 1 eV gap and the absence of magnetic moments and enables one to interpret the crystal structure in terms of orbital ordering [20]. But in the present case when Ti is doped the metal-metal distances increase. That might be reason of interesting behaviour observed in this Ti doped samples.

CONCLUSION:

The magnetization data show that when 10% Mn and Co is doped in ZnV_2O_4 the intensity of peak due to the structural transition goes down. When Mn is doped the resistivity and thermoelectric power increase along with the increase of V-V distance. when Co is doped the V-V separation decreases very slightly, but T_N decreases which suggests that the inter-atomic Coulomb energy U in the localized electron superexchange theory is not constant when Co is doped. The activation energy decreases with the decrease of V-V distance as the metal-insulator transition is approached from the localized-electron side which confirms the reduction of U/t with decrease of V-V distance, which might be due to a partial delocalization of electrons and in this limit neither the localization-electron model and nor the itinerant-electron model is applicable. It is observed from the resistivity curve that at low temperature as the V-V distance decreases the V^{3+} -3d electrons approaches to the Quantum Phase Transition (QPT) from the localized-electron side. Thermally activated behaviour of small polarons for all these vanadates is observed from temperature variation of thermoelectric data. From the variation of $d\chi/dT$ with T plot it is observed that with increase of Mn, that is, with the increase of chemical pressure structural transition is suppressed. Along with T_N , also the charge gap and activation energy of the vanadates depend on the V-V separation and as it decreases a breakdown of localized electron model for the 3d electrons is observed. The XPS study also indicates that with decreasing V-V separation the system moves towards the itinerant electron limit. Ti-doped ZnV_2O_4 samples show some un-usual behaviour. With Ti doping metal-metal distances increase but at the same time T_N increases. It deserves further study to explain the actual mechanism in this Ti doped sample.

Acknowledgement

SC is grateful to DST (Grant No.: SR/S2/CMP-26/2008), CSIR (Grant No.: 03(1142)/09/EMR-II) and BRNS, DAE ((Grant No.: 2013/37P/43/BRNS) for providing financial support. The authors are also grateful to UGC-DAE Consortium for Scientific Research, Indore, India for providing facility for magnetization measurement.

References:

- *Corresponding author *e-mail id:* schatterji.app@iitbhu.ac.in
- [1] Brinkman W F and Rice T M 1970 Phys. Rev. B 2 4302
 - [2] Goodenough J B, Structure and Bonding (springer Verlag Berlin 2001) Vol. 98 chapter 1 & 2

- [3] Blanco-Canosa S, Rivadulla F, Pardo V, Baldomir D, Zhou J S, García-Hernández M, López-Quintela M A, Rivas J and Goodenough J B 2007 Phys. Rev. Lett. 99 187201
- [4] Harrison WA, Electronic structure and the properties of solid: The Physics of the chemical bond (W. H. Freeman & co. San Francisco, 1980)
- [5] Bloch D 1966 J. Phys. Chem. Solids. 27 881
- [6] Zhou J S and Goodenough J B 2002 Phys. Rev. Lett. 89 087201
- [7] Goodenough J B, Longo J M and Kafalas JA 1968 Mater. Res. Bull. 3 471
- [8] Pardo V, Blanco-Canosa S, Rivadulla F, Khomski D I, Bladomir D, Wu H and Rivas J 2008 Phys. Rev. Lett. 101 256403
- [9] Baldomir D, Pardo V, Blanco-Canosa S, Rivadulla F, Rivas J, Piñeiro A and Arias J E 2008 Physica B 403 1639
- [10] untscher C K, Rabia K, Forthaus M K, Abd-Elmeguid M M, Rivadulla F, Kato Y and C.D. Batista 2012 Phys. Rev. B 86 020405(R)
- [11] Tsunetsugu H and Motome Y 2003 Phys. Rev. B 68 060405
- [12] Kato Y, Chern G W, Al-Hassanieh K A, Natalia B P and Batista C D 2012 Phys. Rev. Lett. 108 247215
- [13] Nizioł S 1973 Phys. Status Solidi A18 K11- K13 .
- [14] Rechuis M, Krimmel A, Büttgen N, Loidl A and Prokofiev A 2003 Eur. Phys. J. B 35 311
- [15] Ueda Y, Fujiwara N and Yasuoka H 1997 J. Phys. Soc. Jpn. 66 778
- [16] Niitaka S., Ohsumi H., Sugimoto K., Lee S., Oshima Y., Kato K., Hashizume D., Arima T., Takata M., and Takagi H. 2013 Phys. Rev. Lett. 111 267201
- [17] Takubo K, Son J Y, Mizokawa T, Ueda H, Isobe M, Matsushita Y and Ueda Y 2006 Phys Rev. B 74 155103
- [18] Givonetti G, Stroppa A, Picozzi S, Baldomir D, Pardo V, Blanco-Canosa S, Rivadulla F, Jodlauk S, Niermann D, Rohrkamp J, Lorentz T, Streltsov S, Khomski D I and Hemberger J 2011 Phys. Rev. B 83 060402
- [19] Goodenuogh J B 1982 In proceedings of the climax “4th international conference on chemistry and uses of molybdenum“, edited by H. F. Barry and Mitchell P C H (climax Molybdnum co., Ann Arbor, MI P-1
- [20] Goodenough J B 1971 Solid. State. Chem. 5 145
- [21] Schmidt M, Ratcliff W, Radaelli P G, Refson K, Harrison N M and Cheong S W 2004 Phys. Rev. Lett. 92 056402
- [22] Sawatzky A and Post D 1979 Phys. Rev. B 20 1546
- [23] Maiti K and Sarma D D 2000 Phys. Rev. B 61 2525
- [24] Konstantinović M J, Van den Berghe S, Isobe M and Ueda Y 2005 Phys. Rev. B 72 125124
- [25] Fujimori A, Kawakami K, and Tsuda N 1988 Phys. Rev. B 38 7889
- [26] Matsuno J, Fujimori A and Mattheiss L F 1999 Phys. Rev. B 60 1607 ; Matsuno J, Kobayashi K, Fujimori A, Mattheiss L F and Ueda Y 2000 Physica B 28 281-282
- [27] Harrison W A, Electronic Structure and the Properties of Solid (Dover, New York, 1989).
- [28] Tchernyshyov O 2004 Phys. Rev. Lett. 93 157206
- [29] Khomskii D I and Mizokawa T 2005 Phys. Rev. Lett. 94 156402
- [30] Isobe M and Ueda Y 2002 J. Phys. Soc. Jpn 71 1848-51

Table 1 Structural parameters (lattice parameters, bond lengths) of $Zn_{1-x}A_xV_2O_4$ (with $x=0, 0.05, 0.1$ and $A=Mn, Co, Ti$) samples obtained from Reitveld refinement. The structural data have been refined with Space group I41/a at 10K and Fd-3 m at 300K.

ZnV_2O_4	10 K	a(Å)	5.9481(1)	d(Zn-O)(Å)	4 x 1.96874(4)
		b(Å)	5.9481(1)	d(V-O) (Å)	2x2.00193(7), 4x2.02377(3)
		c(Å)	8.3713(4)	d(V-V)(Å)	2 x 2.96689(6), 4 x 2.97406(7)
	300 K	a(Å)	8.4130(1)	d(Zn-O)(Å)	4 x 1.974774 (3)
				d(V-O) (Å)	6 x 2.01864(3)
				d(V-V)(Å)	6 x 2.97446(3)
$Zn_{0.95}Mn_{0.05}V_2O_4$	10 K	a(Å)	5.9503(3)	d(Zn-O)(Å)	4 x 1.970(6)
		b(Å)	5.9503(3)	d(V-O) (Å)	2 x 2.003(7), 4 x 2.024(4)
		c(Å)	8.3769(2)	d(V-V)(Å)	2 x 2.97517(8), 4 x 2.96843(6)
	300 K	a(Å)	8.4155 (2)	d(Zn-O)(Å)	4 x 1.975359(3)
				d(V-O) (Å)	6 x 2.01924(2)
				d(V-V)(Å)	6 x 2.97534(2)
$Zn_{0.9}Mn_{0.1}V_2O_4$	10 K	a(Å)	5.9540(4)	d(Zn-O)(Å)	4 x 1.97083(8)
		b(Å)	5.9540(4)	d(V-O) (Å)	2 x 2.00432(12), 4 x 2.02578(7)
		c(Å)	8.3813(1)	d(V-V)(Å)	2 x 2.97700(15), 4 x 2.97013(10)
	300 K	a(Å)	8.4174 (1)	d(Zn-O)(Å)	4 x 1.97579(2)
				d(V-O) (Å)	6 x 2.01968(4)
				d(V-V)(Å)	6 x 2.97599(5)
$Zn(V_{0.95}Ti_{0.05})_2O_4$	10 K	a(Å)	5.9487(2)	d(Zn-O)(Å)	4 x 1.96893(5)
		b(Å)	5.9487(2)	d(V-O) (Å)	2 x 2.00210(10), 4 x 2.02398(5)
		c(Å)	8.3719(7)	d(V-V)(Å)	2 x 2.97436(10), 4 x 2.96716(8)
	300 K	a(Å)	8.4115 (6)	d(Zn-O)(Å)	4 x 1.97442(3)
				d(V-O) (Å)	6 x 2.01828(5)
				d(V-V)(Å)	6 x 2.97393(5)
$Zn(V_{0.9}Ti_{0.1})_2O_4$	10 K	a(Å)	5.9487(2)	d(Zn-O)(Å)	4 x 1.96898(8)
		b(Å)	5.9487(2)	d(V-O) (Å)	2 x 2.00227(12), 4 x 2.02398(7)
		c(Å)	8.3726(8)	d(V-V)(Å)	2 x 2.96728(10), 4 x 2.97435(15)
	300 K	a(Å)	8.4102 (7)	d(Zn-O)(Å)	4 x 1.97411(3)
				d(V-O) (Å)	6 x 2.01796(5)
				d(V-V)(Å)	6 x 2.97345(5)
$Zn_{0.9}Co_{0.1}V_2O_4$	10 K	a(Å)	5.9466(2)	d(Zn-O)(Å)	4 x 1.96860(4)
		b(Å)	5.9466(2)	d(V-O) (Å)	2 x 2.00248(7), 4 x 2.02327(4)
		c(Å)	8.3736(1)	d(V-V)(Å)	2 x 2.97331(8), 4 x 2.96692(6)
	300 K	a(Å)	8.4111(9)	d(Zn-O)(Å)	4 x 1.97431(2)
				d(V-O) (Å)	6 x 2.01817(4)
				d(V-V)(Å)	6 x 2.97377(4)

Table 2 Tight-binding parameters for ZnV_2O_4 , $\text{Zn}_{0.9}\text{Mn}_{0.1}\text{V}_2\text{O}_4$ and $\text{Zn}_{0.9}\text{Co}_{0.1}\text{V}_2\text{O}_4$.

Sample		Distance(Å^0)				$\Delta(\text{ev})$		
	Phase	V-V	V-O	$dd\sigma$	$pd\pi$		T_σ	T_π
ZnV_2O_4	Cubic	2.97446	2.01864	-0.4639	0.9321	4.89	-0.3479	-0.1778
	Tetragonal	2.96689, 2.97406	2.02377, 2.00193	-0.4742, -0.4685	0.9305, 0.9666		-0.3557, -0.3514	-0.1771, -0.1911
$\text{Zn}_{0.9}\text{Mn}_{0.1}\text{V}_2\text{O}_4$	Cubic	2.97599	2.01968	-0.4627	0.9304	5.32	-0.3470	-0.1627
	Tetragonal	2.97013, 2.97700	2.02578, 2.00432	-0.4716, -0.4662	0.9237, 0.9625		-0.3537, -0.3497	-0.1604, -0.1741
$\text{Zn}_{0.9}\text{Co}_{0.1}\text{V}_2\text{O}_4$	Cubic	2.97377	2.01817	-0.4645	0.9329	4.79	-0.3484	-0.1817
	Tetragonal	2.96692, 2.97331	2.02327, 2.00248	-0.4741, -0.4691	0.9313, 0.9656		-0.3556, -0.3518	-0.1811, -0.1947

Figure Captions:

1. X-ray diffraction pattern with Reitveld refinement for Mn, Co and Ti doped ZnV_2O_4 samples at (a) 300K and (b) 10K. (c) X-ray diffraction pattern in very narrow 2θ (61.5° - 63°) range at 300K (above the structural transition) and at 10K.
2. Temperature variation of magnetization for $Zn_{1-x}A_xV_2O_4$ [where $x=0.05$ and 0.1 for $A=Mn$ and $x=0.01$ for $A=Co$] spinels at $H=500$ Oe.
3. Variation of T_N with the inverse V-V distance, $1/R_{V-V}$ for the $Zn_{1-x}A_xV_2O_4$ [where $x=0.05$ and 0.1 for $A=Mn$ and $x=0.01$ for $A=Co$] spinels.
4. Temperature dependent Resistivity curves for Mn and Co doped ZnV_2O_4 .
5. Temperature dependent of thermoelectric power for $Zn_{1-x}A_xV_2O_4$ [where $x=0.05$ for $A=Mn$ and $x=0.01$ for $A=Co$].
6. $d\chi/dT$ as a function of Temperature for Mn and Co doped ZnV_2O_4 .
7. Room temperature Absorbance Spectra of $Zn_{1-x}A_xV_2O_4$ [where $x=0.05$ and 0.1 for $A=Mn$ and $x=0.01$ for $A=Co$] and $Zn(V_{1-x}Ti_x)_2O_4$ [where $x=0.05$ and 0.1].
8. Charge gap and activation energy variation as a function of inverse V-V distance for $Zn_{1-x}A_xV_2O_4$ [where $x=0.05$ and 0.1 for $A=Mn$ and $x=0.01$ for $A=Co$].
9. Variation of Volume as a function of $1/R_{V-V}$ for $Zn_{1-x}A_xV_2O_4$ [where $x=0.05$ and 0.1 for $A=Mn$ and $x=0.01$ for $A=Co$].
10. V 2p XPS core-level spectra of ZnV_2O_4 (a), $Zn_{0.9}Mn_{0.1}V_2O_4$ (b) and $Zn_{0.9}Co_{0.1}V_2O_4$ (C); Zn 2p XPS core-level spectra of ZnV_2O_4 (d), $Zn_{0.9}Mn_{0.1}V_2O_4$ (e) and $Zn_{0.9}Co_{0.1}V_2O_4$ (f); Mn 2p XPS core-level spectra of $Zn_{0.9}Mn_{0.1}V_2O_4$ (g); Co 2p XPS core-level spectra of $Zn_{0.9}Co_{0.1}V_2O_4$ (h).
11. Valance-band XPS spectra of ZnV_2O_4 , $Zn_{0.9}Mn_{0.1}V_2O_4$ and $Zn_{0.9}Co_{0.1}V_2O_4$.
12. Temperature variation of magnetization measured at $H=500$ Oe for $Zn(V_{1-x}Ti_x)_2O_4$ [where $x=0.05$ and 0.1].
13. Temperature dependent Resistivity and Seeback Coefficient for $Zn(V_{1-x}Ti_x)_2O_4$ [where $x=0.05$ and 0.1].
14. Variation of Charge gap and Activation energy as a function of $1/R_{V-V}$ for $Zn(V_{1-x}Ti_x)_2O_4$ [where $x=0.05$ and 0.1].

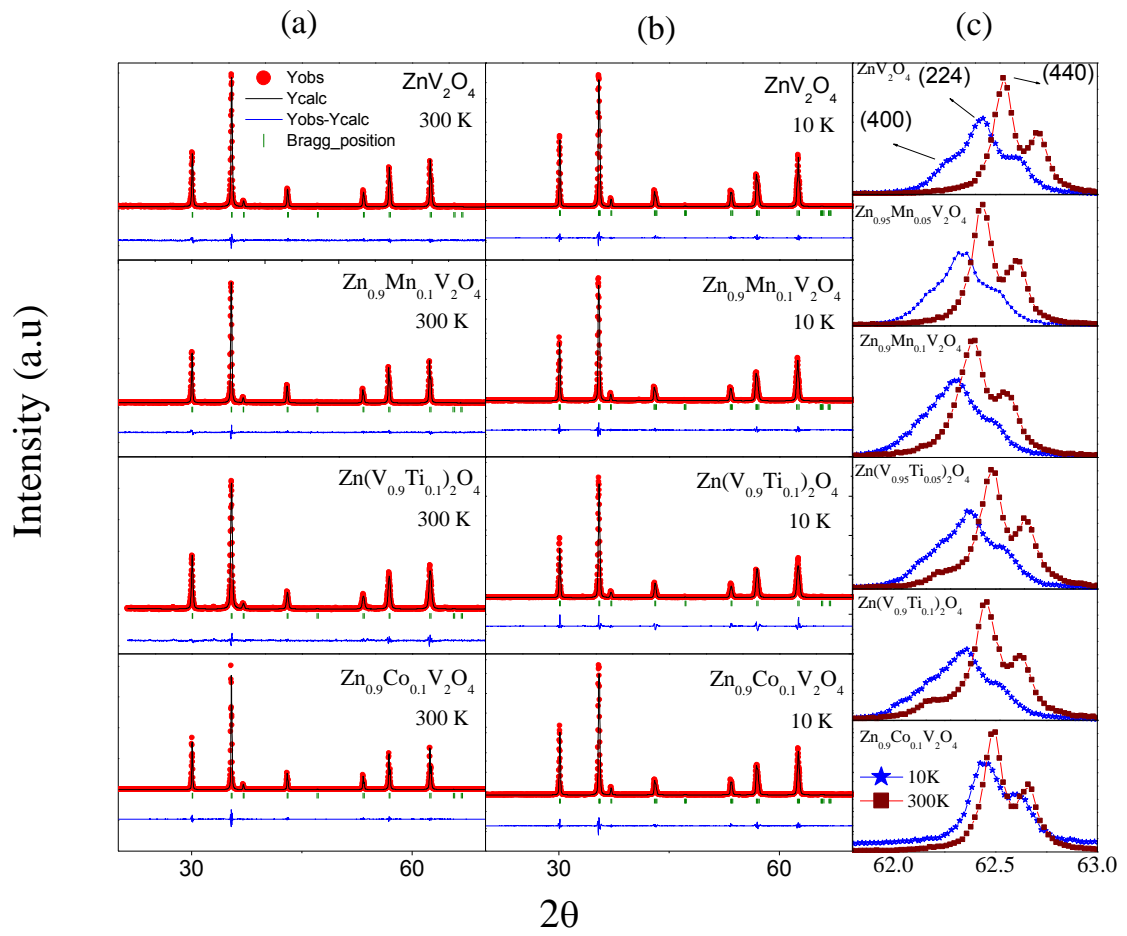


Figure1

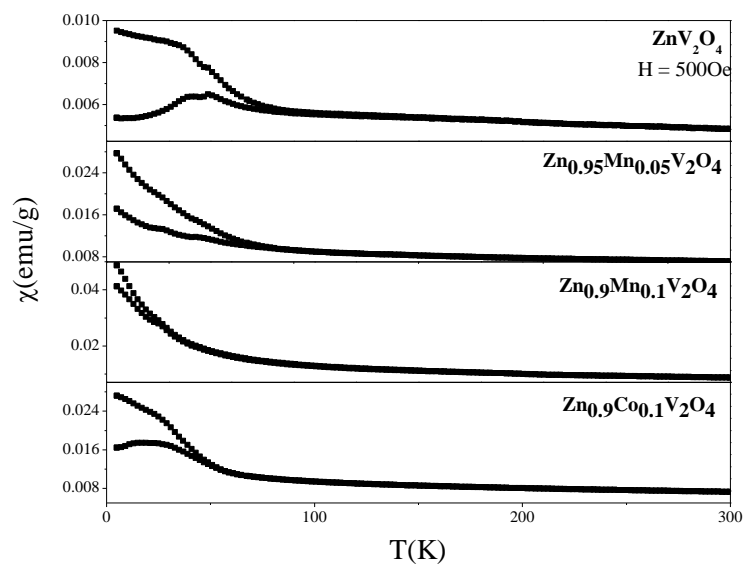


Figure 2

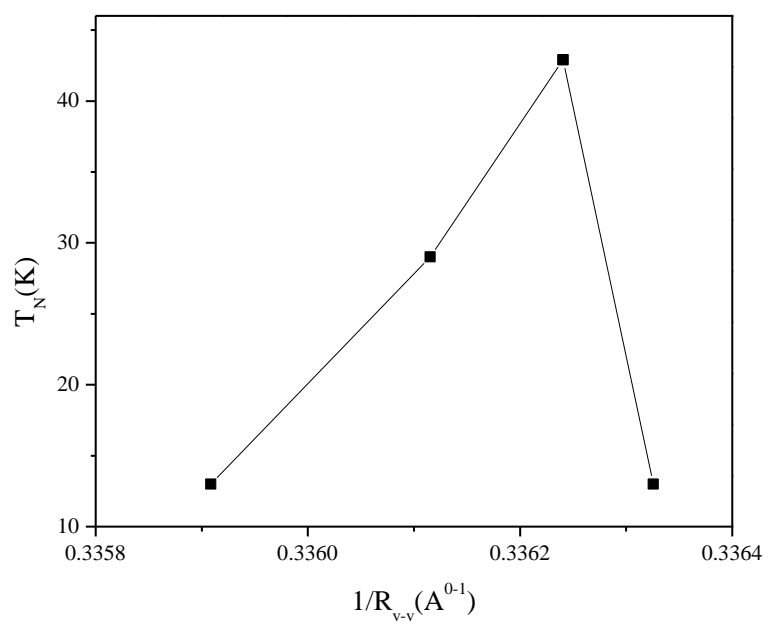


Figure 3

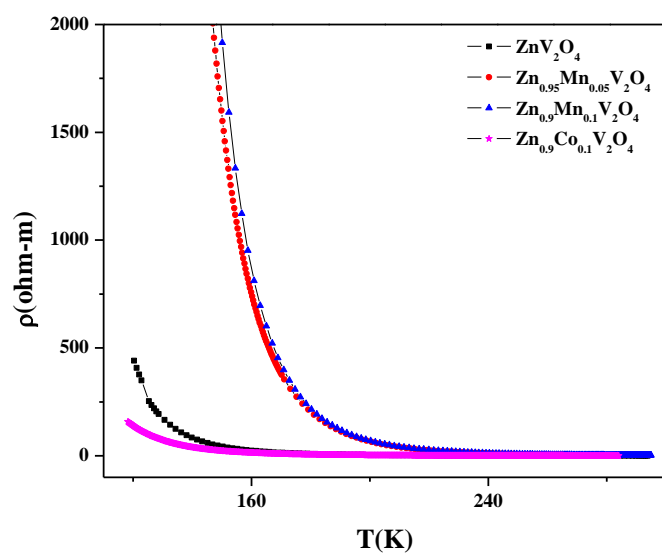


Figure 4

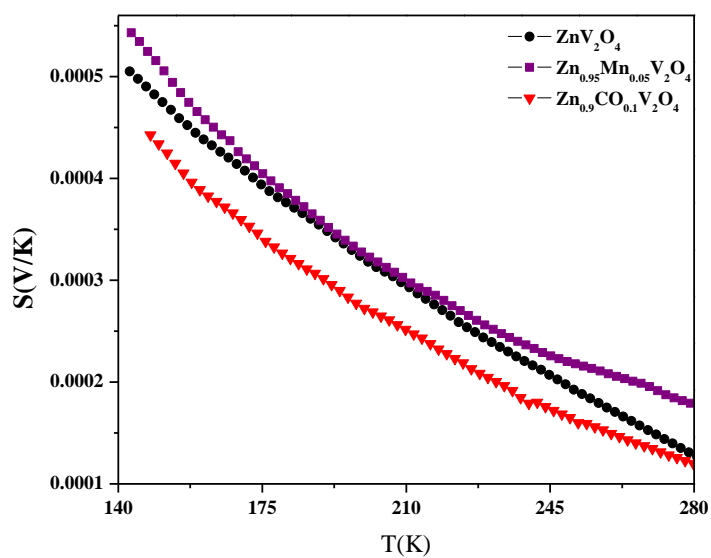


Figure 5

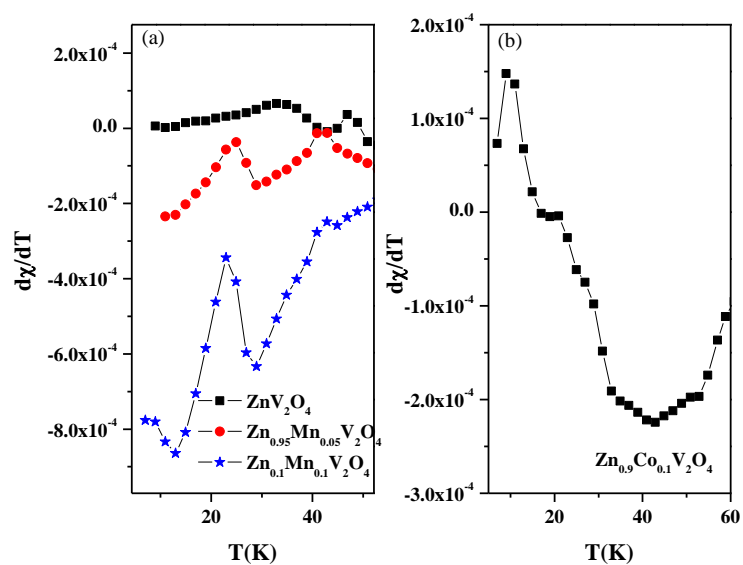


Figure 6

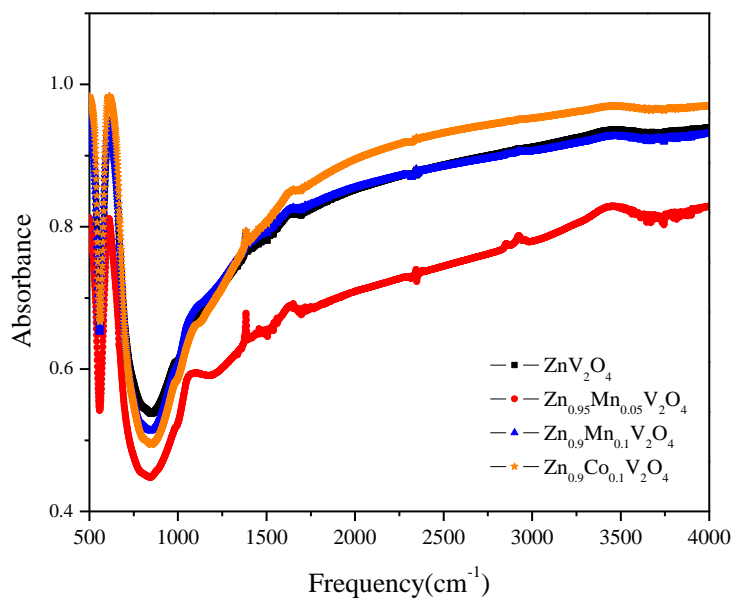


Figure 7

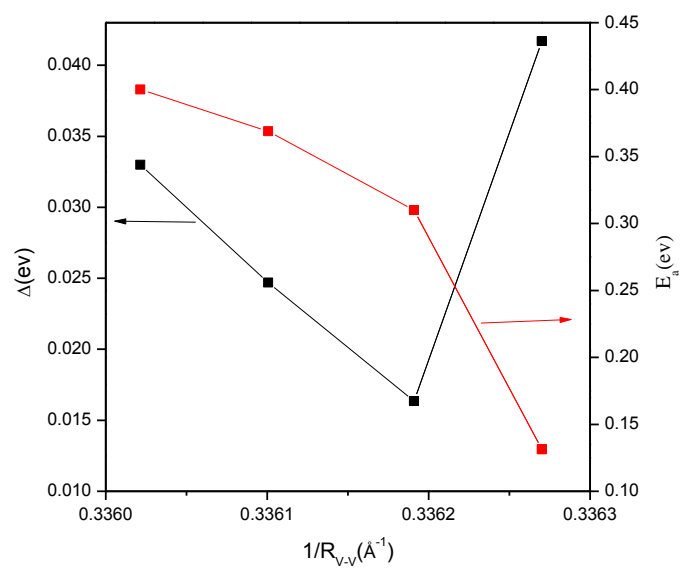


Figure 8

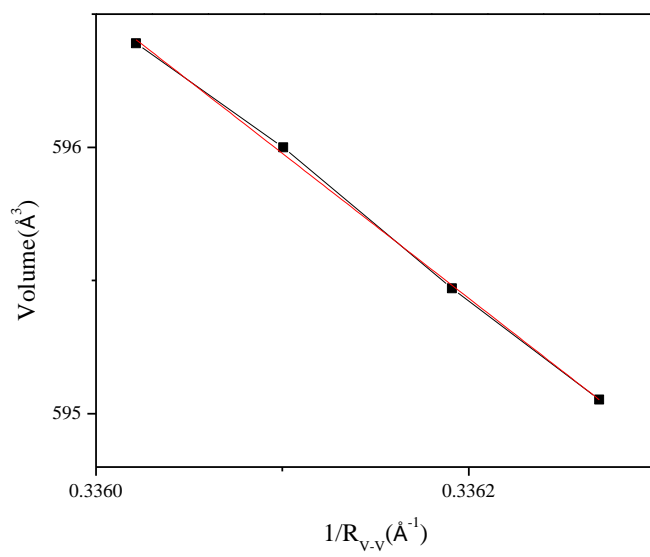


Figure 9

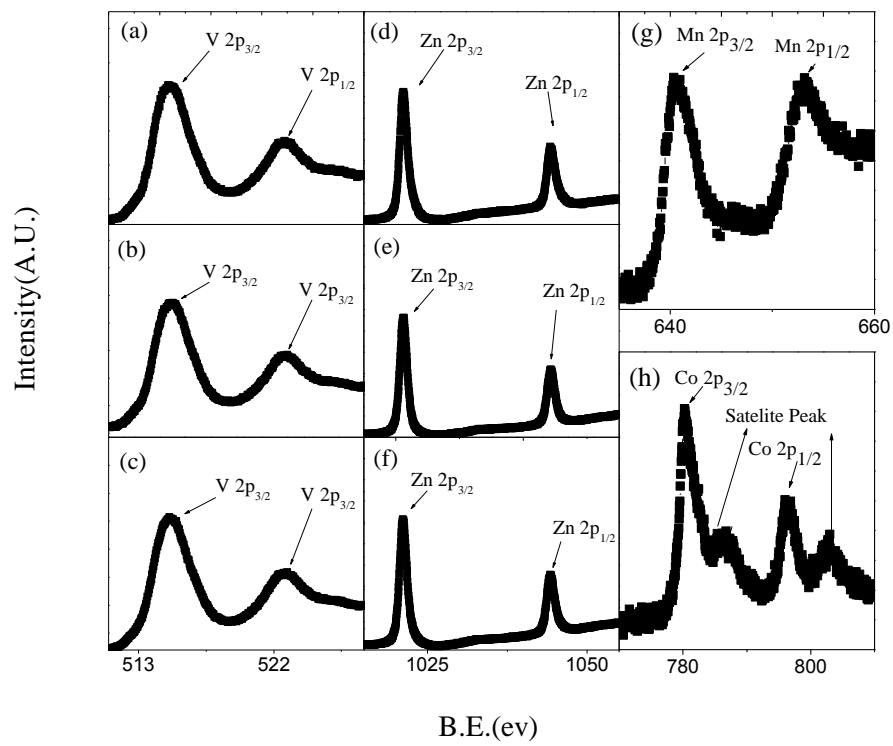


Figure 10

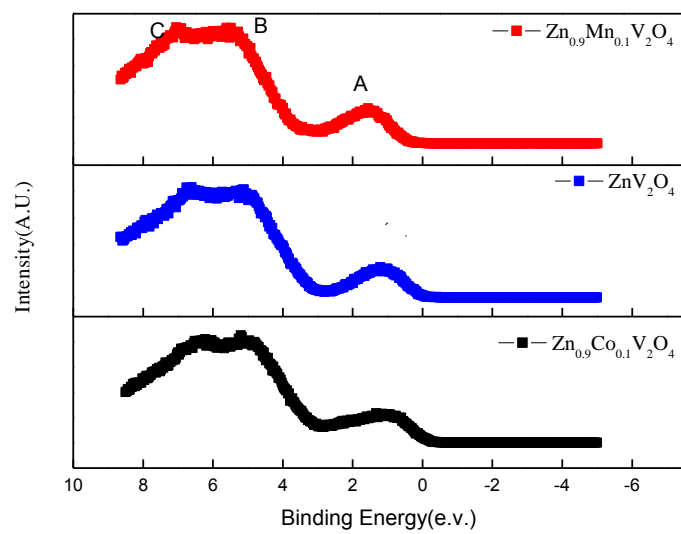


Figure 11

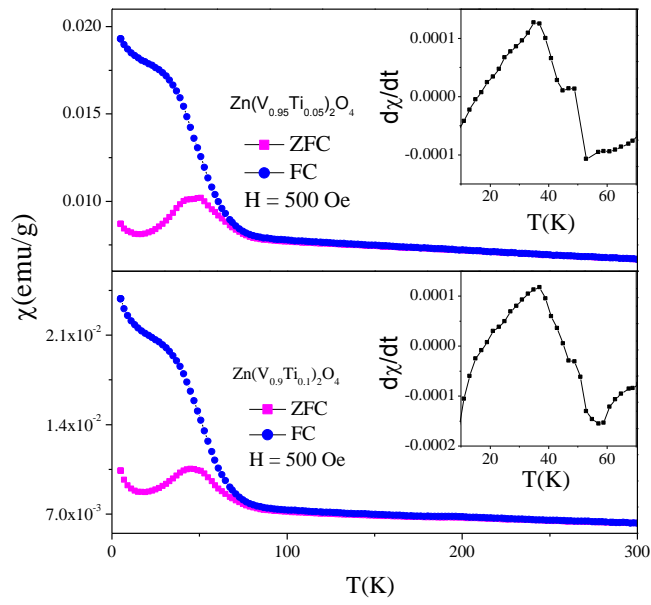


Figure12

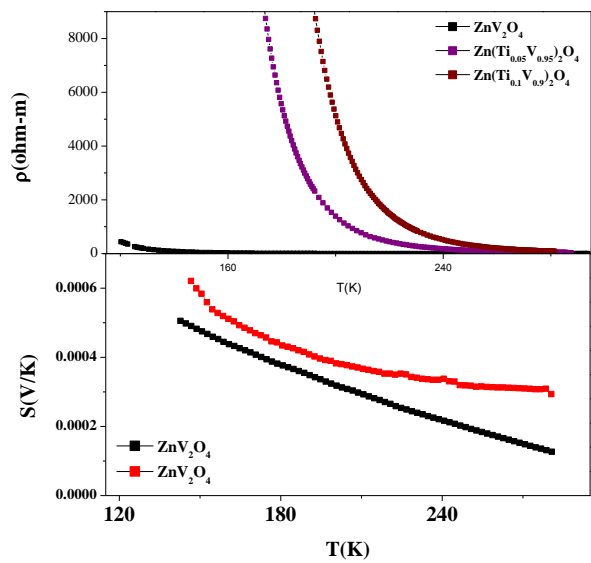


Figure13

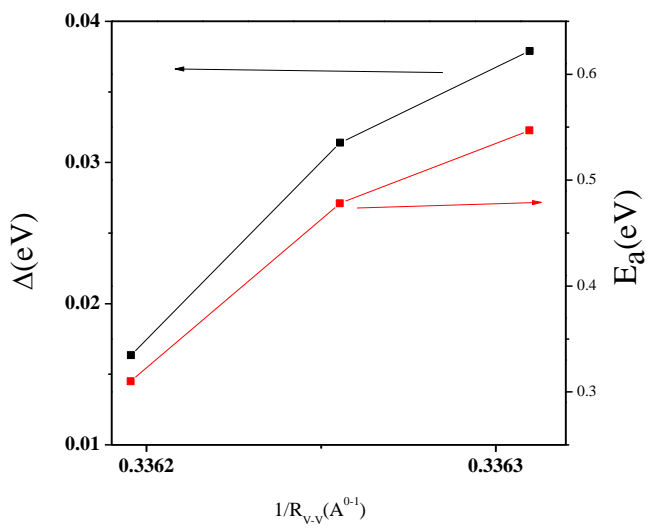


Figure14